

## Structural and optical properties of ZnO nanorods dependence on the molar ratio of zinc acetate dihydrate to hexamethylenetetramine

ChangChun Chen<sup>a,\*</sup>, Nan Ye<sup>a</sup>, ChuanFu YU<sup>b</sup> and Ting FAN<sup>a</sup>

<sup>a</sup>College of Materials Science and Engineering, Nanjing University of Technology, NO.5 Ximofan Road, Nanjing 210009, China

<sup>b</sup>Aerospace Hiwing (Harbin) Titanium industrial Co., Ltd, China

ZnO nanorods were grown on glass substrates coated by an Al-doped ZnO seed layer via a simple solvothermal method using zinc acetate dihydrate ( $\text{Zn}(\text{CH}_3\text{COO})_2 \cdot 2\text{H}_2\text{O}$ ) and Hexamethylenetetramine ( $\text{C}_6\text{H}_{12}\text{N}_4$ ) reagent. The structure, morphology and optical properties of these ZnO nanorods dependence on the molar ratio of  $\text{Zn}(\text{CH}_3\text{COO})_2 \cdot 2\text{H}_2\text{O}$  to  $\text{C}_6\text{H}_{12}\text{N}_4$  were characterized by X-ray diffraction (XRD), scanning electron microscopy (SEM), Ultraviolet and Visible Spectrophotometry (UV-vis) and photoluminescence (PL) spectrometry, respectively. The XRD patterns indicated that all the ZnO nanorods were well-faceted hexagonal structures and preferentially grown along the c-axis. As the molar ratio of  $\text{Zn}(\text{CH}_3\text{COO})_2 \cdot 2\text{H}_2\text{O}$  to  $\text{C}_6\text{H}_{12}\text{N}_4$  decreasing from 2.5 to 0.25, the crystallinity of ZnO nanorods synthesized gradually became inferior and the width of ZnO nanorods also decreased. The blue-shifts of UV emission excited from ZnO nanorods probably arised from the decreased size of ZnO nanorods.

PACS number: 61.10.Nz; 61.46. + w; 78.67.Bf

Key words: ZnO nanorods, Solvothermal, Photoluminescence.

### Introduction

One-dimensional semiconductor nanomaterials have attracted much attention in recent years due to their novel optical, electrical and mechanical properties [1]. Among various one-dimensional semiconductor nanomaterials, Zinc oxide (ZnO) nanorods are the most frequently studied and can be used in nanogenerator [2], rectifying diodes [3], sensors [4], electron emitters and other optoelectronic devices [5] owing to their wide direct bandgap of 3.37 eV and large excitation binding energy of 60 meV at room temperature. Up to now, some methods have been developed to grow well-aligned ZnO nanorods including pulsed laser deposition (PLD) [6], radio frequency (RF) magnetron sputtering [7], plasma enhanced chemical vapor deposition (PECVD) [8], thermal evaporation [9] and templating against anodic alumina membrane [10]. It is worth noting that the above-mentioned methods are expensive and also require a high-growth temperature with complex experimental conditions. Consequently, searching a simple, low-temperature and low cost methodology to synthesize aligned ZnO nanorods array is of great importance for both fundamental study and practical application. Fortunately, an aqueous solution process such as hydrothermal (HT) [11] or Sol-gel [12] has become the

subject of interest in the growth of ZnO nanorods. Especially, effect of ZnO nanorod growth on seed layer has been reported by a hydrothermal method [13] or by Sol-gel method [12, 14]. However, only zinc nitrate hexahydrate [ $\text{Zn}(\text{NO}_3)_2 \cdot 6\text{H}_2\text{O}$ ] and hexamethylenetetramine (HMT) [ $\text{C}_6\text{H}_{12}\text{N}_4$ ] have been used for the hydrothermal or Sol-gel growth of ZnO nanorods in previous literature.

In this study, zinc acetate dihydrate [ $\text{Zn}(\text{CH}_3\text{COO})_2 \cdot 2\text{H}_2\text{O}$ ] together with HMT was used as raw material to synthesize ZnO nanorods via a simple solvothermal method. The dependence of ZnO nanorods on the molar ratio of zinc acetate dihydrate to HMT were thoroughly discussed. The crystal structures and surface morphologies of ZnO nanorods were measured by XRD and SEM. The optical performances of the ZnO nanorods were characterized by an UV-Vis absorption spectra spectrophotometer together with a photoluminescence (PL) spectrometer.

### Experimental Procedure

All chemicals were reagent grade and used without further purification: zinc acetate dihydrate [ $\text{Zn}(\text{CH}_3\text{COO})_2 \cdot 2\text{H}_2\text{O}$ , Beijing Chemical Reagent Co.] and hexamethylenetetramine [ $\text{C}_6\text{H}_{12}\text{N}_4$ , Tianjin Chemical Reagent Co.]. Glass plates were used as substrates and were cleaned to remove contaminants by standard procedures prior to use. ZnO nanorod array films were coated on a glass substrate by a two-step method. A thin Al-doped ZnO seed buffer layer was first deposited via a Sol-gel method, and then a ZnO nanorod array

\*Corresponding author:  
Tel : +86-02583587242  
Fax: +86-02583587242  
E-mail: changchunchen@hotmail.com

film was grown via a solvothermal method. An Al-doped ZnO thin film used as a seed layer was ascribed to its characteristic of transparent conductive oxide (TCO) such as high transparency, stability and high conductivity and the existence of an Al-doped ZnO seed layer could improve the uniformity and orientation of the ZnO nanorod arrays formed. The growth process of Al-doped ZnO seed layer was detailedly described in our previous work [15].

$\text{Zn}(\text{CH}_3\text{COO})_2 \cdot 2\text{H}_2\text{O}$  and HMT reagents were separately dissolved into deionized water at room temperature, respectively. The concentrations of  $\text{Zn}(\text{CH}_3\text{COO})_2 \cdot 2\text{H}_2\text{O}$  aqueous solutions were adjusted at 0.025 mol/l. The concentrations of HMT aqueous solutions were adjusted at 0.001 mol/l, 0.025 mol/l, 0.05 mol/l, and 0.1 mol/l, respectively. That is to say, the molar concentration ratios of  $\text{Zn}(\text{CH}_3\text{COO})_2 \cdot 2\text{H}_2\text{O}$  to HMT reagents were 2.5, 1, 0.5, and 0.25, respectively. After uniformly stirred, we mixed and continuously agitated them for 30 minutes. And then, we transferred them into four Teflon-line autoclaves. Four glass substrates coated with the identical Al-doped ZnO seed layer were loaded on Teflon holder in an autoclave, respectively. The seeded surface was faced to bottom of container, and the holder was immersed into the reagent solution. The container was finally covered using a commercially fabricated Teflon lead to avoid the evaporation. During the growth of ZnO nanorods, these four Teflon-line autoclaves were placed into an electric oven at a temperature of 90 °C. After keeping temperature at 90 °C for three hours, the vessels were cooled down to room temperature naturally. The products on substrate were washed with deionized water and ethanol for several times and dried them in an electric oven at a temperature of 90 °C for two hours.

The crystal structures of ZnO nanorod films synthesized in this study were investigated by  $\theta$ - $2\theta$  method of XRD with a  $\text{Cu K}\alpha_1$  ( $\lambda = 0.15406$  nm) source at 40 kV and 30 mA using a multi-purpose XRD system (D/MAX-RB). The morphologies of the ZnO nanorod films were also analyzed by a scanning electron microscope (SEM, JSM-5900). The SEM photographs for the ZnO nanorod films were recorded at 15 kV from samples covered with gold thin films. The optical properties and crystal defects of the ZnO nanorod films were obtained through room temperature photoluminescence using an excitation wavelength of 325 nm via a Horiba Jobin Yvon FL3-221 spectrometer. Optical absorption was examined on a UV2102PCS UV-vis spectrophotometer.

## Results and Discussion

Phase identification of the synthesized ZnO nanorods was done with XRD analysis. Fig. 1 shows the XRD patterns of four kinds of ZnO nanorods synthesized by

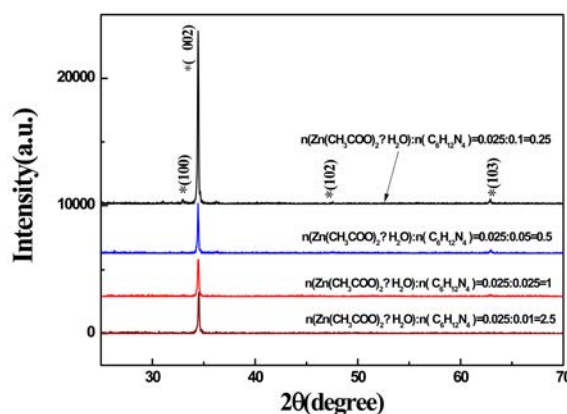


**Fig. 1.** XRD patterns of four kinds of ZnO nanorods synthesized by the precursors of  $\text{Zn}(\text{CH}_3\text{COO})_2 \cdot 2\text{H}_2\text{O}$  and  $\text{C}_6\text{H}_{12}\text{N}_4$  with the molar concentration ratio at 2.5, 1.0, 0.5, and 0.25, respectively.

the precursors of  $\text{Zn}(\text{CH}_3\text{COO})_2 \cdot 2\text{H}_2\text{O}$  and HMT with the molar concentration ratio at 2.5, 1, 0.5, and 0.25, respectively. All the diffraction peaks can be indexed within experimental error as hexagonal ZnO phase (wurtzite structure) and space group,  $P6_3mc$  by comparison with the data from the Joint Committee on Powder Diffraction Standard (JCPDS) card for ZnO (JCPDS 36-1451) [16]. The clear and narrow diffraction peaks in Fig. 1 indicate that all the ZnO nanorods have a highly preferential orientation growth along c-axis and further evidence that ZnO nanorods tend to grow perpendicular to the Al-doped ZnO seed layer surface. It should be pointed out that as the molar ratio of Zinc acetate dihydrate to Hexamethylenetetramine reagents decreasing from 2.5 to 0.25, the relative intensity of (002) diffraction peak detected from ZnO nanorods becomes stronger and diffraction peaks from (100), (102) and (103) planes of ZnO nanorod also appear in XRD patterns.

The morphologies of ZnO nanorods were examined by SEM. Fig. 2 (a-d) shows the SEM plain-view images of four kinds of ZnO nanorods synthesized by the precursors of  $\text{Zn}(\text{CH}_3\text{COO})_2 \cdot 2\text{H}_2\text{O}$  and HMT with the molar concentration ratio at 2.5, 1, 0.5, and 0.25, respectively. As seen from these images, the grown ZnO layers have high density of clear well-faceted hexagonal nanorod structures that are of well-arranged growth direction, which are consistent with these XRD results. The normal direction of (0 0 2) plane of ZnO nanorod is vertical to the Al-doped ZnO seed layer. That is, approximate directional 1D (one dimensional) growth along the c-axis of ZnO nanorods is realized on the glass substrate. As the molar ratio of  $\text{Zn}(\text{CH}_3\text{COO})_2 \cdot 2\text{H}_2\text{O}$  to HMT reagents decreasing from 2.5 to 0.25, the diameter of ZnO nanorod also decreased. The reason that the width of ZnO nanorod decreased as the molar ratio of  $\text{Zn}(\text{CH}_3\text{COO})_2 \cdot 2\text{H}_2\text{O}$  to HMT reagents decreasing from 2.5 to 0.25 could be explained as follows. ZnO is a well-known amphoteric oxide. During the growth of ZnO nanorods by the

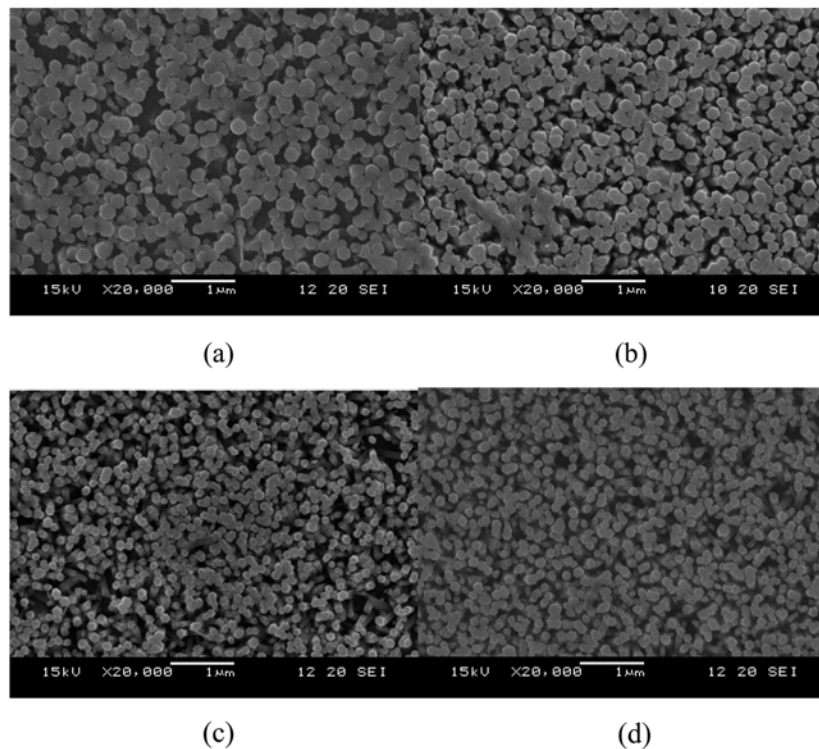


**Fig. 2.** SEM images of four kinds of ZnO nanorods synthesized by the precursors of  $\text{Zn}(\text{CH}_3\text{COO})_2 \cdot 2\text{H}_2\text{O}$  and  $\text{C}_6\text{H}_{12}\text{N}_4$  with the molar concentration ratio at 2.5, 1.0, 0.5, and 0.25, respectively.

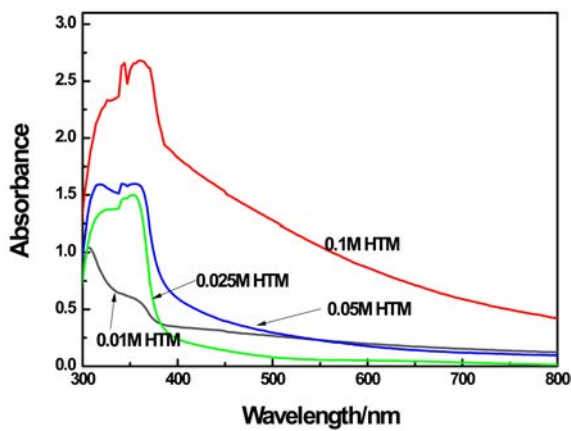


**Fig. 3.** UV-Vis absorption spectra of four kinds of ZnO nanorods synthesized by the precursors of  $\text{Zn}(\text{CH}_3\text{COO})_2 \cdot 2\text{H}_2\text{O}$  and  $\text{C}_6\text{H}_{12}\text{N}_4$  with the molar concentration ratio at 2.5, 1.0, 0.5, and 0.25, respectively.

precursors of  $\text{Zn}(\text{CH}_3\text{COO})_2 \cdot 2\text{H}_2\text{O}$  and HMT, the higher molar ratio of HMT to  $\text{Zn}(\text{CH}_3\text{COO})_2 \cdot 2\text{H}_2\text{O}$  reagents could result in higher pH of the precursor solution. The high pH of the precursor solution is responsible for the preferential hexagonal ZnO etching and thus parts of ZnO nanorods are dissolved, which is also reported in the literature [17].

The UV-vis absorption spectra of the ZnO nanorods synthesized by the precursors of  $\text{Zn}(\text{CH}_3\text{COO})_2 \cdot 2\text{H}_2\text{O}$  and HMT with the molar concentration ratio at 2.5, 1.0, 0.5, and 0.25 are given in Fig. 3. All the absorption spectra of ZnO nanorods in this study show broad

exciton band with the wavelength between 300 and 400 nm and blue-shifted relative to the bulk exciton absorption (378 nm), which mainly originates from the free carrier or excitonic transition between the valence band and the conduction band. With a decrease of molar concentration of  $\text{Zn}(\text{CH}_3\text{COO})_2 \cdot 2\text{H}_2\text{O}$  to HMT from 2.5 to 0.25, the absorption intensity of the exciton band gradually becomes large. In addition, the lower light absorption in the visible spectral range shown in Fig. 3 suggests that more absorption states or defect's energy bands exist in the synthesized ZnO nanorods.

The optical properties of the ZnO nanorods synthesized in this study are also examined by room temperature photoluminescence, as shown in Fig. 4. All the PL spectra of ZnO nanorods exhibit a typical ultraviolet (UV) emission and a relatively broad visible emission in the range of 470-630 nm. By comparison, it can be found that with a decrease of the molar concentration ratio of  $\text{Zn}(\text{CH}_3\text{COO})_2 \cdot 2\text{H}_2\text{O}$  to HMT from 2.5 to 0.25, there are three obvious changes in the PL spectra of the ZnO nanorods: (i) the emission intensity in UV region of ZnO nanorods declines; (ii) the position of emission peak blue-shifts towards shorter wavelength in UV region; and (iii) the luminescence intensity in the visible emission region remarkably enhances. It is well-established that for the ZnO, the UV emission at 378 nm originates from the radical recombination of free excitations [18]. The blue-shift of the UV emission is attributed to the quantum confinement effect, and this phenomenon is probably due to the small size of

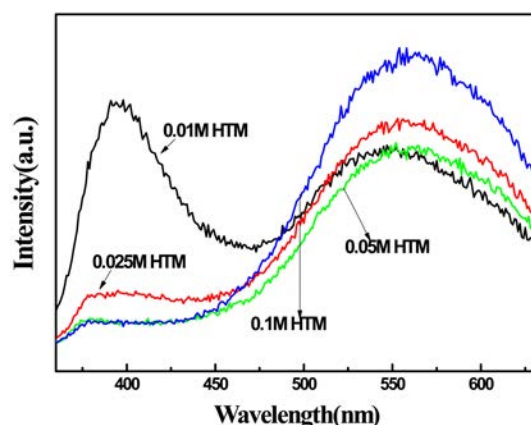


**Fig. 4.** Room-temperature photoluminescence spectra for four kinds of ZnO nanorods synthesized by the precursors of  $\text{Zn}(\text{CH}_3\text{COO})_2 \cdot 2\text{H}_2\text{O}$  and  $\text{C}_6\text{H}_{12}\text{N}_4$  with the molar concentration ratio at 2.5, 1.0, 0.5, and 0.25, respectively.

the ZnO nanorods, which can be seen from SEM images in Fig. 2. The origins of the visible emission peaks in the range of 470-630 nm are generally attributed to the structural defects such as the singly ionized oxygen vacancies and the interstitials of the ZnO, which were usually observed in the oxygen-rich film or nanomaterials [19-21]. In addition, the intensity ratio of UV to visible emissions can be used to evaluate the quality of ZnO nanorods [22]. The intensity ratio of UV to visible emissions for the ZnO nanorod grown by the precursor of  $\text{Zn}(\text{CH}_3\text{COO})_2 \cdot 2\text{H}_2\text{O}$  and HMT with the molar concentration ratio at 2.5 of is largest, and thus the crystallinity of ZnO nanorod also should be best, which is validated by XRD patterns and SEM images, respectively. On the other hand, smaller-size ZnO nanorods shown in Fig. 2 correspond to a lower intensity ratio of UV to visible emissions (shown in Fig. 4) due to a larger surface area-to-volume ratio and more surface defects [23]. Consequently, the ZnO nanorod arrays grown with higher  $\text{C}_6\text{H}_{12}\text{N}_4$  concentration are of an UV-blocking property.

## Conclusions

In summary, Well-defined ZnO nanorod arrays with hexagonal structure have been successfully prepared by a solvothermal method. The as-grown ZnO arrays show well orientation growth with the c-axis of ZnO vertical to the glass substrates coated by an Al-doped ZnO seed layer. The crystallinity and width of as-grown ZnO nanorods would change via changing the  $\text{Zn}(\text{CH}_3\text{COO})_2 \cdot 2\text{H}_2\text{O}$  and HMT concentration. With a decrease of the molar concentration ratio of  $\text{Zn}(\text{CH}_3\text{COO})_2 \cdot 2\text{H}_2\text{O}$  to  $\text{C}_6\text{H}_{12}\text{N}_4$  from 2.5 to 0.5, the intensity of the exciton band of ZnO nanorods determined by UV-Vis absorption spectra gradually augments and the width of ZnO nanorods also decreases owing to ZnO etching in higher pH of the precursor solution. All the PL spectra ZnO nanorods

exhibit a typical ultraviolet (UV) emission and a relatively broad visible emission in the range of 470-630 nm. Blue-shift of the UV emission excited from ZnO nanorods was probably ascribed to the decreased size of the ZnO nanorods. On the other hand, the intensity of UV emission from the ZnO nanorods synthesized by the higher molar ratio of HMT to  $\text{Zn}(\text{CH}_3\text{COO})_2 \cdot 2\text{H}_2\text{O}$  also becomes smaller. This work not only simplifies the preparation procedure of ZnO nanorods arrays with low cost for large-scale fabrication, but also provides an easier way to realize ultraviolet emission (UV)-blocking property.

## Acknowledgments

This study is partially financed by the Priority Academic Program Development of Jiangsu Higher Education Institutions (PAPD), China.

## References

1. D.C. Look, Recent advances in ZnO materials and devices, *Mater. Sci. Eng. B* 80 (2001) 383-387.
2. Z.L. Wang, J. Song, Piezoelectric Nanogenerators Based on Zinc Oxide Nanowire Arrays, *Science*. 312 (2006) 242-246.
3. C.S. Lao, J. Liu, P.X. Gao, L. Zhang, D. Davidovic, R. Tummala and Z.L. Wang, ZnO Nanobelt/Nanowire Schottky Diodes Formed by Dielectrophoresis Alignment across Au Electrodes, *Nano Lett.* 6 (2006) 263-266.
4. C.S. Rout, S. Harikrishna, S.R.C. Vivekchand, A. Govindaraj and C.N.R. Rao, Hydrogen and ethanol sensors based on ZnO nanorods, nanowires and nanotubes, *Chem. Phys. Lett.* 418 (2006) 586-591.
5. D.Pradhan, M. Kumar, Y. Ando, K.T. Leung, One-dimensional and two-dimensional ZnO nanostructure materials on a plastic substrate and their field emission properties, *J. Phys. Chem. C Letters*. 112 (2008) 7093-7096.
6. T. Okada, B. H. Agung, Y. Nakata, ZnO nano-rods synthesized by nano-particle-assisted pulsed-laser deposition, *Appl. Phys. A* 79 (2004) 1417-1419.
7. C. Li, M. Furuta, T. Matsuda, T. Hiramatsu, H. Furuta, T. Hirao, Effects of substrate on the structural, electrical and optical properties of Al-doped ZnO films prepared by radio frequency magnetron sputtering, *Thin Solid Films*. 517 [11] (2009) 3265-3268.
8. D. Wang, H. W. Seo, C.-C. Tin, M. J. Bozack, J. R. Williams, M. Park, N. Sathitsuksanoh, An-jen Cheng, and Y. H. Tzeng, Effects of postgrowth annealing treatment on the photoluminescence of zinc oxide nanorods, *J. Appl. Phys.* 99 (2006) 113509-113513.
9. J.H. Zheng, Q. Jiang, J.S. Lian, Synthesis and optical properties of ZnO nanorods on indium tin oxide substrate, *Applied Surface Science*. 258 (2011) 93-97.
10. J.T.Yan, C.H.Chen, S.F.Yen, C.T.Lee, Ultraviolet ZnO nanorod/P-GaN-heterostructured light-emitting diodes, *IEEE Photonics Technol. Lett.* 22 (2010) 146-148.
11. Seong Jong Kim, Han Hyoung Kim, Joo Beom Kwon, Jong Geun Lee, Beom Hoan O, Seung Gol Lee, El-Hang Lee, Se-Geun Park, Novel fabrication of various size ZnO nanorods using hydrothermal method, *Microelectronic Engineering*. 87 (2010) 1534-1536.
12. K.Prabakar, Heeje Kim, Growth control of ZnO nanorod

- density by sol-gel method, *Thin Solid Films*. 518 (2010) e136-e138.
13. Seong-Jong Kim, Han-Hyoung Kim, Joo-Beom Kwona, Jong-Geun Lee, Beom-Hoan O, Seung Gol Lee, El-Hang Lee, Se-Geun Park, Novel fabrication of various size ZnO nanorods using hydrothermal method, *Microelectronic Engineering*, 87 (2010) 1534-1536.
  14. S.J. Kwon, J.H. Park, J.G. Park, *Appl. Phys. Lett.* 87 (2005) 133112.
  15. N. Huang, M.W. Zhu, L.J. Gao, J. Gong, C. Sun, X. Jiang, A template-free sol-gel technique for controlled growth of ZnO nanorod arrays., *Applied Surface Science*. 257 [14] (2011) 6026-6033.
  16. Nan Ye, Chang Chun Chen, Investigation of ZnO nanorods synthesized by a solvothermal method, using Al-doped ZnO seed films, *Optical Materials*. 34 (2012) 753-756.
  17. A. Khorsand Zak, M. Ebrahimizadeh Abrishami, W.H. Abd. Majid, Ramin Yousefi, S.M. Hosseini, Effects of annealing temperature on some structural and optical properties of ZnO nanoparticles prepared by a modified sol-gel combustion method., *Ceramics International*. 37 [1] (2011) 393-398.
  18. Michael Breeedon, Colin Rix, Kourosh Kalantar-zadeh, seeded growth of ZnO nanorods from NaOH solutions, *Materials Letters*. 63 (2009) 249-251.
  19. R.A. Laudise, A.A. Ballman, Hydrothermal synthesis of zinc oxide and zinc sulfide, *J. Phys. Chem.* 64 (1960) 688-691.
  20. R. Yousefi, B. Kamaluddin, Fabrication and characterization of ZnO and ZnMgO nanostructures grown using a ZnO/ZnMgO compound as the source material, *Appl. Sur. Sci.* 256 (2009) 329-334.
  21. L. Wu, Y. Wu, X. Pan, F. Kong, Synthesis of ZnO nanorod and the annealing effect on its photoluminescence property, *Opt. mater.* 28 (2006) 418-422.
  22. L.H. Quang, S.J. Chua, K.P. Loh, E. Fitzgerald, The effect of post-annealing treatment on photoluminescence of ZnO nanorods prepared by hydrothermal synthesis, *J. Cryst. Growth*. 287 (2006) 157-161.
  23. M. Izaki, S. Watase, and H. Takahashi, Room-temperature ultraviolet light-emitting zinc oxide micropatterns prepared by low-temperature electrodeposition and photoresist., *Appl. Phys. Lett.* 83 [24] (2003) 4930-4932.
  24. Q. Tang, W. Zhou, J. Shen, W. Zhang, L. Kong, Y. Qian, A template-free aqueous route to ZnO nanorod arrays with high optical property., *Chem. Commun.* 10 [6] (2004) 712-713.